Fish and Shellfish Immunology 88 (2019) 318–327

Contents lists available at ScienceDirect

Fish and Shellfish Immunology

journal homepage: www.elsevier.com/locate/fsi

Full length article

# A novel LRR and Ig domain-containing protein could function as an immune effector in *Crassostrea gigas*

Xiudan Wang[a], Xiaoli Zhao[a], Chunyu Yan[a], Zhihao Jia[b,c], Zhao Lv[b,d], Cuiping Ma[a], Mengqiang Wang[b,e,f,g,*]

[a] Shandong Provincial Key Laboratory of Biochemical Engineering, College of Marine Science and Biological Engineering, Qingdao University of Science and Technology, Qingdao, 266042, China
[b] CAS Key Laboratory of Experimental Marine Biology, Institute of Oceanology, Chinese Academy of Sciences, Qingdao, 266071, China
[c] Department of Animal Sciences, Purdue University, IN, 47907, USA
[d] University of Chinese Academy of Sciences, Beijing, 100049, China
[e] Research Platform for Marine Molecular Biotechnology, National Laboratory for Marine Science and Technology, Qingdao, 266237, China
[f] Laboratory for Marine Biology and Biotechnology, National Laboratory for Marine Science and Technology, Qingdao, 266237, China
[g] CAS Center for Ocean Mega-Science, Chinese Academy of Sciences, Qingdao, 266400, China

ARTICLE INFO

*Keywords:*
*Crassostrea gigas*
Leucine-rich repeat domain
Immunoglobulin domain
LRRIG
Pattern recognition receptor
Immune effector

ABSTRACT

A variety of combinations of leucine-rich repeat (LRR) and immunoglobulin-like (Ig) domains have been found and discovered in invertebrates and vertebrates, but the functions remain largely unexplored. In the present study, a novel LRR and Ig domain-containing protein (LRRIG), CgLRRIG-3, was identified and characterized from oyster *Crassostrea gigas*. It contained two typical LRR motifs, a LRRNT motif and an Ig domain and PSI-BALST and phylogeny analysis revealed that the sequence of CgLRRIG-3 was most related with leucine-rich repeat neuronal 1 proteins from vertebrate. Its mRNA transcripts were constitutively expressed in muscle, gill, hepatopancreas, mantle, gonad and hemocytes with the highest level in hepatopancreas. The mRNA expression level of CgLRRIG-3 in hemocytes could respond to the stimulations of variety PAMPs including lipopolysaccharide (LPS), peptidoglycan (PGN), glucan (GLU) and polyinosinic-polycytidylic acid (poly I:C). The recombinant proteins exhibited a wide PAMP binding repertoire to four typical PAMPs and could significantly induce the expression of CgTNF-1 and CgIL17-5 as well as increase phagocytosis in primary cultured oyster hemocytes. In hepatopancreas, CgLRRIG-3 was mainly distributed in the basolateral membrane of digestive tubule and the hemocoel sinusoid between the digestive tubules. And in hemocytes, the positive signal was mainly distributed in a special group of granulocytes. These results collectively indicated that CgLRRIG-3 could not only function as an immune effector.

## 1. Introduction

The innate immune system is the first line of defense against pathogens and it entails sensing various pathogen associated molecular patterns (PAMPs) via different pattern recognition receptors (PRRs), which then initiate downstream signal pathways [1,2]. Various combinations of protein domains constitute to the receptors of innate immunity including leucine-rich repeat (LRR) domain, immunoglobulin-like (Ig) domain, caspase-recruitment domain, lectin domain and so on [3–6]. LRR domain and Ig domain have been found in a diverse set of proteins, which could mediate ligand recognition and induce immune responses against pathogens [1,2].

LRR domain usually contains 2–45 tandem LRR motifs, each of which is 20–29 residues in length, containing a motif of LxxLxLxxN/CxL [3,7]. These repeats could form a characteristic horse-shoe structure, providing molecular basis for binding to various PRRs [3]. For both vertebrates and invertebrates, LRR containing proteins have been reported to mediate protein-protein or protein-ligand interaction and play important roles in immune responses [8,9]. For example, Toll-like receptors (TLRs) are characterized by extracellular LRR domain and intracellular Toll/IL-1 receptor (TIR) domain, and mediate the TLR signaling pathways in innate immune defense [10]. Cytoplasmic nucleotide-binding oligomerization domain-like receptors (NLRs) family is also featured with C-terminal LRR domain and plays key roles in PAMP recognition and downstream signal transduction [11]. In recent years, the immune functions of proteins containing merely LRR domain

* Corresponding author. CAS Key Laboratory of Experimental Marine Biology, Institute of Oceanology, Chinese Academy of Sciences, Qingdao, 266071, China.
*E-mail address:* wangmengqiang@qdio.ac.cn (M. Wang).

https://doi.org/10.1016/j.fsi.2019.03.003
Received 26 October 2018; Received in revised form 26 February 2019; Accepted 1 March 2019
Available online 07 March 2019
1050-4648/ 

(LRR-only proteins) have also been verified in a variety of invertebrates such as scallop, amphioxus and so on [12–14]. Two LRR-only proteins from scallop *Chlamys farreri* (CfLRRop1 and CfLRRop3) could function as PRRs and were demonstrated to bind various PAMPs including LPS, PGN, GLU and poly I:C [12,13]. Ig domain containing proteins serve extensive functions in direct recognition of ligands, cell adhesion, and signal transduction [15,16]. In vertebrates, the diversified forms of Ig protein are the central structural features of adaptive immune responses [15]. In invertebrates, Ig superfamily (IgSF) could combine with a series of domains and participate in various immune defenses. For example, one or two N-terminal IgSF domains and a C terminal fibrinogen (FBG) domain could form a diverse family of fibrinogen related proteins (FREPs) involved in internal defense in snail [17]. In *Crassostrea gigas*, one N-terminal V-set Ig domain, C2-set Ig domains and cytosolic immunoreceptor tyrosine-based inhibitory motifs (ITIMs) composed sialic acid binding immunoglobulin-type lectin (siglec), which modulated the immune responses such as cell apoptosis and phagocytosis [18].

A typical LRR and Ig domain containing-protein (LRRIG) consists an N-terminal LRR region, one or more central Ig domains, a transmembrane region, and a C-terminal cytoplasmic tail [14]. In recent years, a series of LRRIGs have been identified and some of them were found to be functioned. For example, the human leucine-rich repeats and immunoglobulin-like domains (LRIG, named by Gene Nomenclature Committee) gene family were illustrated to contain three members, LRIG1, LRIG2, and LRIG3, and they were suggested to play important functions in many cell types and organs [19,20]. In invertebrates, approximate 20 LRRIG models could be found in the sea urchin genome and 240 LRRIG models in the amphioxus genome, demonstrating the prevalence of LRRIGs [14]. In Drosophila, some LRRIGs named kekkon were revealed to be regulated by epidermal growth factor receptor (EGFR) [21,22]. However, compared to the large amount of LRRIG proteins in invertebrates, the functions of LRRIGs in invertebrates still remain largely unexplored. As both LRR and Ig motifs are competent immune recognition modules, the biological activities, cell distribution and immunological relevance of LRRIGs are worth investigating.

The Pacific oyster *C. gigas* is one of the most important species worldwide and considerable attention has been paid on its immune system against complex environment in the estuaries and intertidal zones [23]. In the course of long-term evolution, oysters have developed diversified PRRs, including peptidoglycan recognition proteins (PGRPs), TLRs, lectins, gram-negative binding proteins (GNBPs), fibrinogen-related proteins (FREPs) and so on [24]. In our previous research, two novel LRRIGs, CgLRRIG-1 and CgLRRIG-2, which are of the same origin, was identified in *C. gigas* [25]. Our results demonstrated that these two proteins could be regarded as a new type of PRR in oyster. However, compared to other oyster PRRs, more information are still needed to illustrate the exact roles of LRRIGs and deepen our understanding about the immune system of oyster. In the present study, a novel LRRIG (designated as CgLRRIG-3) has been identified in *C. gigas*, with the main purposes to, 1) investigate the response pattern of CgLRRIG-3 mRNA in hemocytes post different PAMPs stimulation, 2) study the PAMP binding activity and possible pro-inflammatory activity of its recombinant proteins, 3) characterize its distribution in hemocytes and explore its potential immunological function in innate immunity, hopefully to make contributions to the further understanding the cellular immunity and humoral immunity in oyster.

## 2. Materials and methods

### 2.1. Oysters, immune stimulation and sample collection

Adult oysters *C. gigas* with an average 13.0 cm in shell length were collected from a local farm in Qingdao, China and were pre-punched by the side of shell and then maintained at 20 °C in the aerated seawater for one week. Approximately 300 oysters were employed for PAMPs stimulation assay. Four different PAMPs including PGN (77140, Fluck, USA), LPS (L2630, Sigma Aldrich, USA), GLU (G5011, Sigma Aldrich, USA), and poly I:C (P1530, Sigma Aldrich, USA) were used for immune stimulation. The oysters in each group received an injection of 100 μL PGN, LPS, GLU, poly I:C in PBS with concentration of 0.5 mg $mL^{-1}$. Oysters in the control group received an injection of 100 μL PBS. The hemolymphs from five individual oysters were collected at 3, 6, 9, 12, 24 and 48 h post injection and centrifuged at 800 *g*, 4 °C for 10 min to harvest the hemocytes. Muscle, gill, hepatopancreas, mantle, female gonad, male the gonad and hemocytes of five untreated oysters were collected to determine mRNA transcripts of CgLRRIG-3.

**Table 1**
Primers used in this work.

| Primers | Sequence (5′-3′) |
|---|---|
| Oligo(dT)-adaptor | GGCCACGCGTCGACTAGTACT$_{17}$ |
| CgLRRIG-3-F | ATGCCACTGTTGTTTTACCTC |
| CgLRRIG-3-R | TTACACTGAACTTTGAGCTACTAT |
| M13-47 | CGCCAGGGTTTTCCCAGTCACGAC |
| RV-M | GAGCGGATAACAATTTCACACAGG |
| CgLRRIG-3-qRT-F | TGATGGAGACCACCCTCCCAA |
| CgLRRIG-3-qRT-R | CAATGGGCCAGCGCATGGTT |
| CgEF-qRT-F | AGTCACCAAGGCTGCACAGAAAG |
| CgEF-qRT-R | TCCGACGTATTTCTTTGCGATGT |
| CgLRRIG-3-recombinant-F | GATATCATGCCACTGTTGTTTTACCTCA |
| CgLRRIG-3-recombinant-R | GAATTCCAAACTGAATATCTTGACGTCCAC |
| CgTNF-1-qRT-F | CTTCTCGTCTGCGGCTTCTTT |
| CgTNF-1-qRT-R | CAGGGCTGCGGTCTTTCC |
| CgIL17-5-qRT-F | CGTCCTTGCCTTACTGACTAGA |
| CgIL17-5-qRT-R | TGTCGTTGTCCTCTACCATGAT |

### 2.2. RNA isolation and cDNA synthesis

The total RNA of different tissues was isolated using traditional Trizol-chloroform method. The first strand synthesis of cDNA was performed with M-MLV reverse transcriptase using the DNase I (M6101, Promega, USA) treated RNA as template and oligo (dT)-adaptor as primer (Table 1). The reaction was carried out at 42 °C for 1 h and terminated at 95 °C for 5 min. The obtained cDNA mixture was diluted 40-fold and stored at −80 °C for subsequent quantitative real-time PCR (qRT-PCR).

### 2.3. cDNA cloning of CgLRRIG-3

The cDNA sequence of CgLRRIG-3 (JH816453.1) was obtained from the National Center for Biotechnology Information (NCBI, http://www.ncbi.nlm.nih.gov/). One pair of primers, CgLRRIG-3-F and CgLRRIG-3-R, were designed to clone the cDNA sequence. The PCR products were inserted into pMD 19-T simple vector (6013, TaKaRa, Japan), transformed into *Escherichia coli* trans5α (CD201, TransGen, China) and confirmed by DNA sequencing with pMD19-T simple vector primers M13-47 and RV-M. The primers used were listed in Table 1.

### 2.4. Sequence features and phylogeny analysis

The cDNA sequence and deduced amino acid sequence of *Cg*LRRIG-3 was analyzed using the BLAST algorithm (http://www.ncbi.nlm.nih.gov/blast). LRR motifs were predicted by LRRFinder 2.0 (http://www.lrrfinder.com). Ig domains were determined using the Simple Modular Architecture Research Tool (SMART, http://smart.embl-heidelberg.de/). The theoretical isoelectric point and molecular mass was calculated using ExPASy ProtParam tool (https://web.expasy.org/protparam/). BLAST and PSI-BLAST algorithms were used to search for sequences related to *Cg*LRRIG-3. Phylogenetic analysis of 13 sequences revealed by PSI-BLAST was performed with Poisson model in Mega 5.0 by Neighbor-Joining methods.

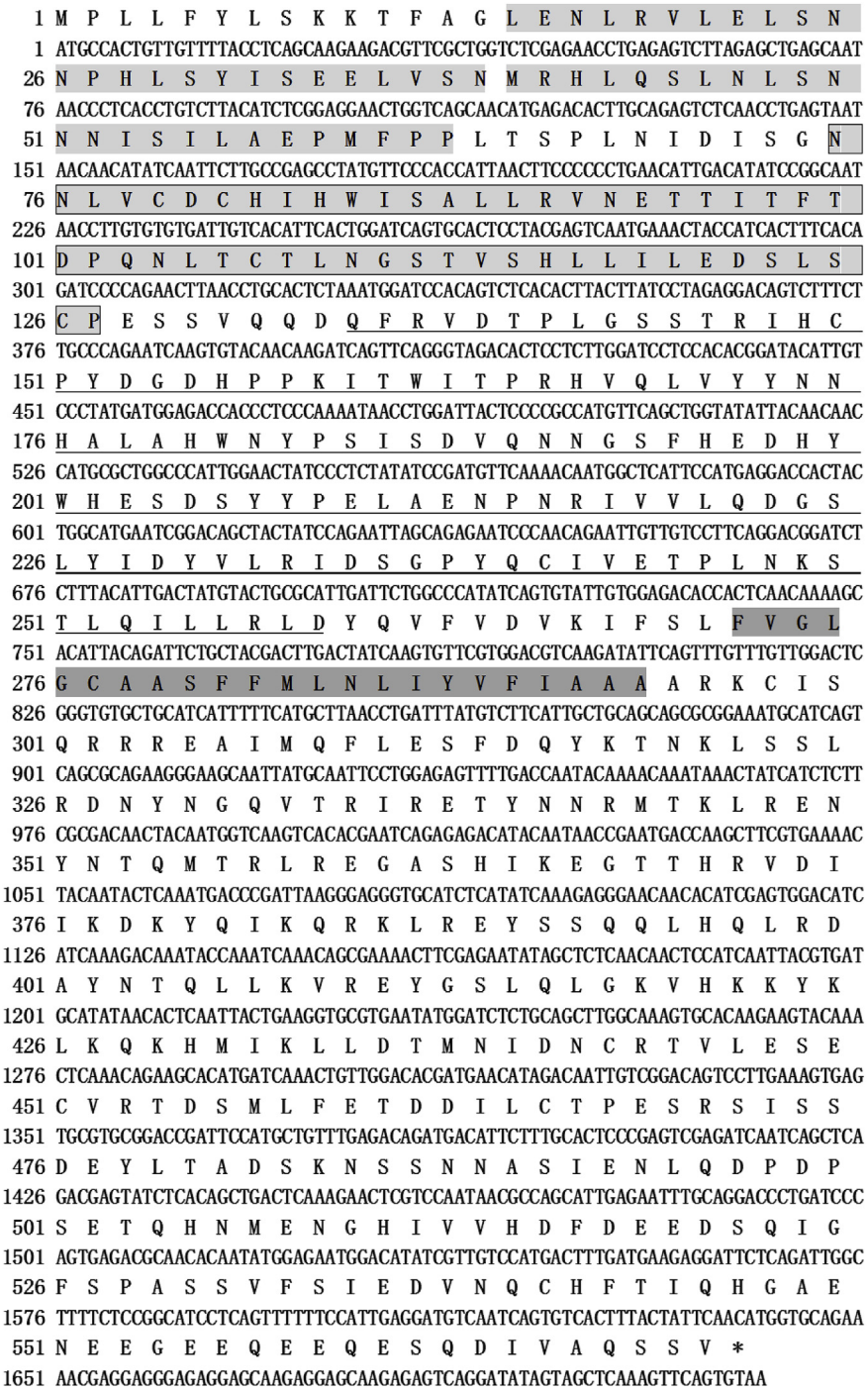


**Fig. 1.** Nucleotide and deduced amino acid sequences of CgLRRIG-3. The LRR motifs were in light grey shade, the LRRNT motif was in light grey with rectangular circle, the Ig domains were underlined, and the transmembrane domain was in grey shade.

### *2.5. qRT-PCR analysis of the mRNA expression level of CgLRRIG-3*

The relative mRNA expression levels of *Cg*LRRIG-3 in different tissues were detected by qRT-PCR with SYBR Premix Ex Taq (Tli RNaseH Plus) (RR420A, Takara, Japan). One pair of specific primers, *Cg*LRRIG-3-qRT-F and *Cg*LRRIG-3-qRT-R were used to amplify fragments of 87 bp. The *C. gigas* elongation factor 1α (*Cg*EF) fragment amplified with primers *Cg*EF-qRT-F and *Cg*EF-qRT-R (Table 1) was used as the internal control. The mRNA expression level of *Cg*LRRIG-3 was determined by $2^{-\Delta\Delta Ct}$ method. The female gonad was used as the reference tissue to determine the mRNA distributions of *Cg*LRRIG-3 in different tissues. For determination of the temporal mRNA expression profile of *Cg*LRRIG-3 after stimulation, the 0 h was used as the reference time.

### *2.6. Recombinant expression of CgLRRIG-3 and preparation of polyclonal antibody*

One pair of primers, CgLRRIG-3-recombinant-F and CgLRRIG-3-recombinant-R, with EcoR V and EcoR I enzyme sites were designed for amplification of LRR repeats and Ig domain of CgLRRIG-3 (protein sequence: $M_1$-$L_{271}$). The amplified PCR fragments and expression vector pMAL-c5X were digested with EcoR V and EcoR I enzymes and purified with fragments purification kit (9761, TaKaRa, Japan). The digested fragments of CgLRRIG-3 and pMAL-c5X were connected to obtain the

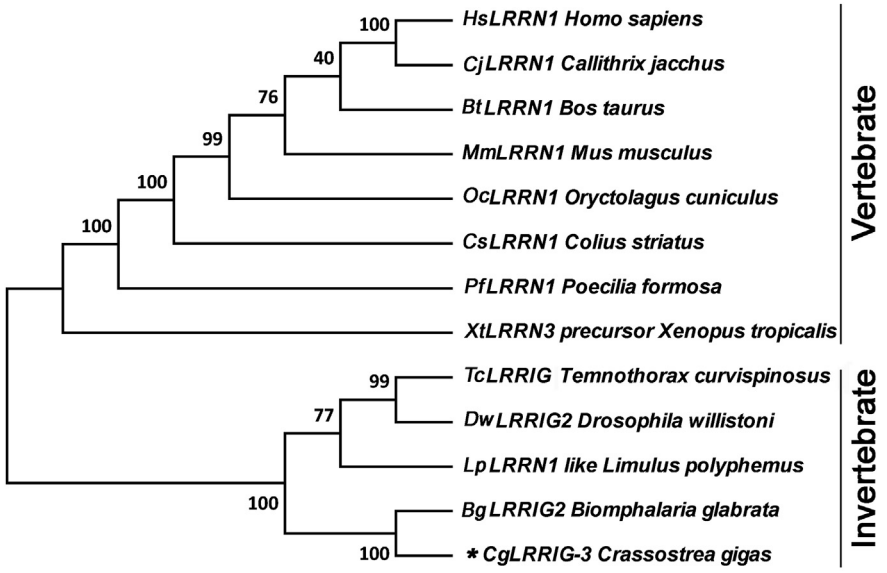


**Fig. 2.** Phylogenetic tree of CgLRRIG-3 and other genes obtained by PSI-BLAST algorithms. The numbers at the forks indicated the bootstrap value. The following twelve sequences including Leucine rich repeat neuronal 1 (LRRN1) of *Homo sapiens* (*Hs*LRRN1) (AAH34947.1), LRRN1 of *Callithrix jacchus* (*Cj*LRRN1) (XP_008980301.1), LRRN1 of *Bos taurus* (*Bt*LRRN1) (XP_005222725.1), LRRN1 of *Mus musculus* (*Mm*LRRN1) (AAH31122.1), LRRN1 of *Oryctolagus cuniculus* (*Oc*LRRN1) (XP_002720661.2), LRRN1 of *Colius striatus* (*Cs*LRRN1) (XP_010199400.1), LRRN1 of *Poecilia formosa* (*Pf*LRRN1) (XP_007566133.1), LRRN3 of *Xenopus tropicalis* (*Xt*LRRN3) (NP_001072526.1), leucine-rich repeat and immunoglobulin-like domain-containing nogo receptor-interacting protein 2 of *Temnothorax curvispinosus* (*Tc*LRRIG2) (XP_024889695.1), immunoglobulin domain and leucine-rich repeat-containing protein 2 *Drosophila willistoni* (*Dw*LRRIG2) (XP_002064633.1), LRRN1 of *Limulus polyphemus* (*Lp*LRRN1) (XP_022253919.1), immunoglobulin domain and leucine-rich repeat-containing protein 2 of *Biomphalaria glabrata* (*Bg*LRRIG2) (XP_013062202.1) were selected for phylogenetic analysis by Neighbor-Joining methods with Poisson model in Mega 5.0. The reliability of the branching was tested using bootstrap of 1000.

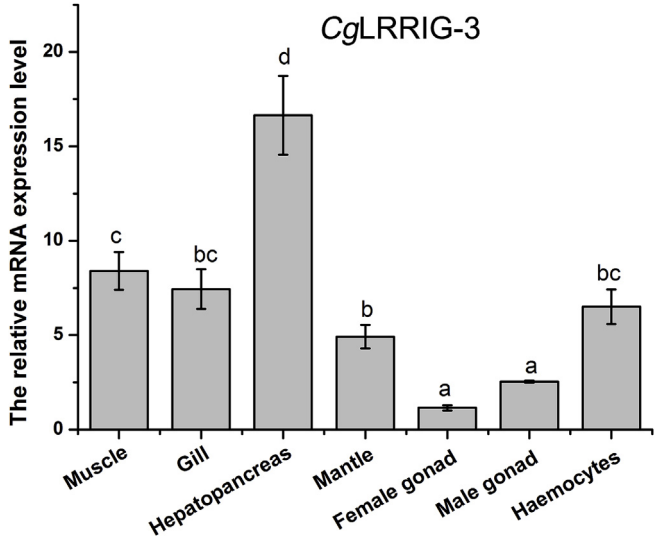


**Fig. 3.** Tissue distribution of CgLRRIG-3 mRNA transcripts detected by qRT-PCR. CgEF gene was used as an internal control. The mRNA expression level of CgLRRIG-3 in muscle, gill, hepatopancreas, mantle, male gonad and hemocytes was normalized to that of female male gonad. The results were shown as mean ± S.D. (n = 3), and bars with different characters indicated significantly different ($p < 0.05$).

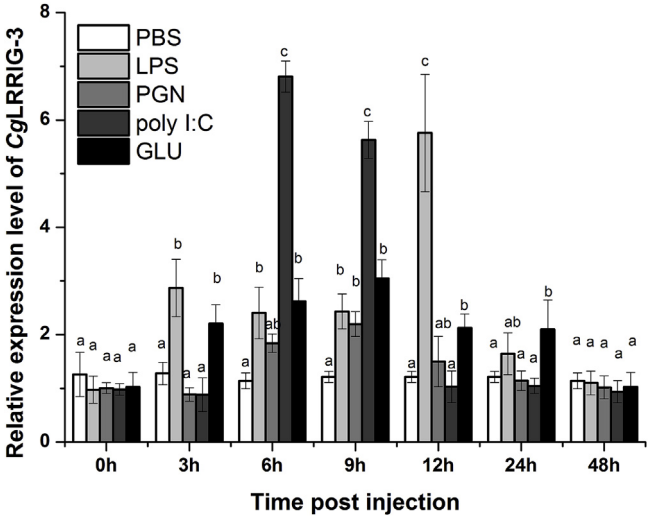


**Fig. 4.** Temporal mRNA expression profiles of CgLRRIG-3 detected by qRT-PCR in oyster hemocytes at 0, 3, 6, 9, 12, 24 and 48 h post LPS, PGN, poly I:C and GLU stimulation. The results were shown as mean ± S.D. (n = 3), and bars with different characters indicated significantly different ($p < 0.05$).

recombinant plasmids pMAL-c5X-CgLRRIG-3. The recombinant plasmids and pMAL-c5X vector were transformed into *E. coli* transetta (DE3) (CD801, TransGen, China) to obtain a maltose binding protein (MBP) tagged CgLRRIG-3 protein (rCgLRRIG-3) and a MBP, respectively. The two proteins were induced and purified according to our previous study [26]. The resultant protein was separated by reducing 12% Sodium Dodecyl Sulphate - Poly Acrylamide Gel Electrophoresis (SDS-PAGE), and visualized with coomassie brilliant blue R-250. The concentrations of purified rCgLRRIG-3 and MBP were quantified by an enhanced bicinchonininc acid (BCA) kit (P1101, Beyotime, China) and stored at −80 °C.

### 2.7. Preparation of a polyclonal antibody and western blotting

The polyclonal antibodies of rCgLRRIG-3 was prepared by immunizing female mice as described previously [26]. The serum of immunized mice was harvested and used as the polyclonal antibody in following western blotting and immunohistochemistry. The western blotting of the rCgLRRIG-3 in hemocytes and hepatopancreas was performed according to the previous report [27].

### 2.8. ELISA based PAMPs binding assay

The activity of rCgLRRIG-3 towards four different PAMPs including LPS, PGN, poly I:C and GLU were examined by enzyme linked immune sorbent assay (ELISA) according to the previous description [12]. Briefly, 100 μL PAMP solution (0.1 mg $mL^{-1}$ in $Na_2CO_3$—$NaHCO_3$ buffer) was coated to a 96-well microtiter plate at 4 °C overnight. After washing and blocking, 100 μL of rCgLRRIG-3 and MBP with different concentrations in 0.1 mg $mL^{-1}$ BSA were incubated at 37 °C for 1 h. Then the plate was washed and incubated with 100 μL MBP polyclonal antibody (A00190, Genscript, 1:1000) at 37 °C for 1 h. After that, the plate was incubated with 100 μL goat-anti-mouse Ig-HRP conjugates

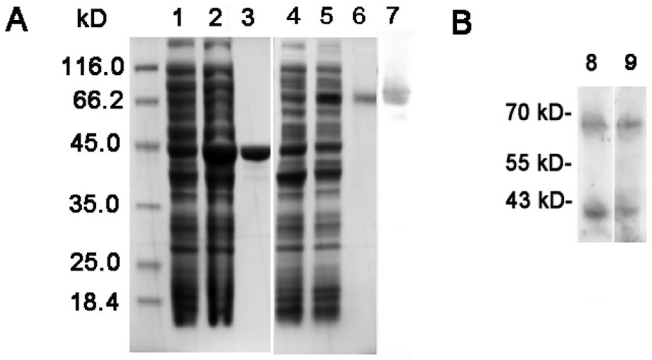


**Fig. 5.** A. SDS-PAGE and western blotting analysis of rMBP and rCgLRRIG-3. B. Western blotting of CgLRRIG-3 in hepatopancreas and hemocytes. Lane M: protein molecular standard; Lane 1, 4: the supernatant of non-induced bacteria lysate; Lane 2, 5: the supernatant of IPTG-induced rMBP, and rCgLRRIG-3; Lane 3, 6,: purified rMBP, and rCgLRRIG-3; Lane 7: western blotting analysis of the polyclonal antibody against rCgLRRIG-3; Lane 8, 9: western blotting analysis of the polyclonal antibody against CgLRRIG-3 in hepatopancreas and hemocytes.

(AS003, Abclonal, 1:2000) as the secondary antibody at 37 °C for 1 h. The following procedures were the same as previous study [28] and each experiment was repeated in triplicate.

### 2.9. Hemocyte primary culture and stimulation experiment

The primary culture of oyster hemocytes was performed according to previous study [25]. Briefly, hemolymphs from twenty oysters were withdrawn from adductor muscle sinus and 400 μL of them were added to each well of a 24-well flat bottom plate. After 3-h attachment, the upper fluids were drawn out and 400 μL modified Leibovitz's L-15 mediums (supplemented with 0.54 g $L^{-1}$ KCl, 20.2 g $L^{-1}$ NaCl, 1.0 g $L^{-1}$ $MgSO_4$, 0.6 g $L^{-1}$ $CaCl_2$, 3.9 g $L^{-1}$ $MgCl_2$, 20.8 g $L^{-1}$ glucose, 10% fetal calf serum pH 7.0, M-L-15) was added into each well. Then the hemocytes were treated with 50 μL TBS (Tris-HCl buffer, pH = 7.40), MBP and rCgLRRIG-3, respectively and incubated at 21 °C, 5% $CO_2$ for 12 h. Finally, the hemocytes were harvested to determine phagocytosis rate and the expression levels of CgTNF-1 (tumor necrosis factor of *C. gigas*) and CgIL17-5 (interleukin 17 of *C. gigas*) after incubation. RT-PCR primers of CgTNF-1 and CgIL17-5 (CgTNF-1-qRT-F and CgTNF-1-qRT-R, CgIL17-5-qRT-F and CgIL17-5-qRT-R) were adopted according to previous reports [29,30].

### 2.10. Flow cytometry assay of phagocytosis rate

Primarily cultured hemocytes were collected and analyzed by a FACS Arial II flow cytometer (Becton Dickinson Biosciences). Rate of phagocytosis was determined using FITC-labeled latex beads (L4530, Sigma, USA) according to previous study [25]. Hemocytes were incubated with the beads at a ratio of 100:1 at room temperature for 1 h with rotation. Then the cells were washed with M-L-15 medium and phagocytosis rate was determined with FSC and FL1 channel.

### 2.11. Immunohistochemistry of CgLRRIG-3 in hemycytes and hepatopancreas

The immunohistochemistry of CgLRRIG-3 in hemocytes and hepatopancreas was performed according to previous reports [26,28]. Hemolymphs from twenty oysters were withdrawn from adductor muscle sinus and quickly centrifuged at 800 × *g* at 4 °C for 10 min to collect the hemocytes. The hemocytes were suspended with M-L-15 medium and the obtained suspension was added onto positively charged slides and incubated for 3 h. Then the supernatant was discarded and the

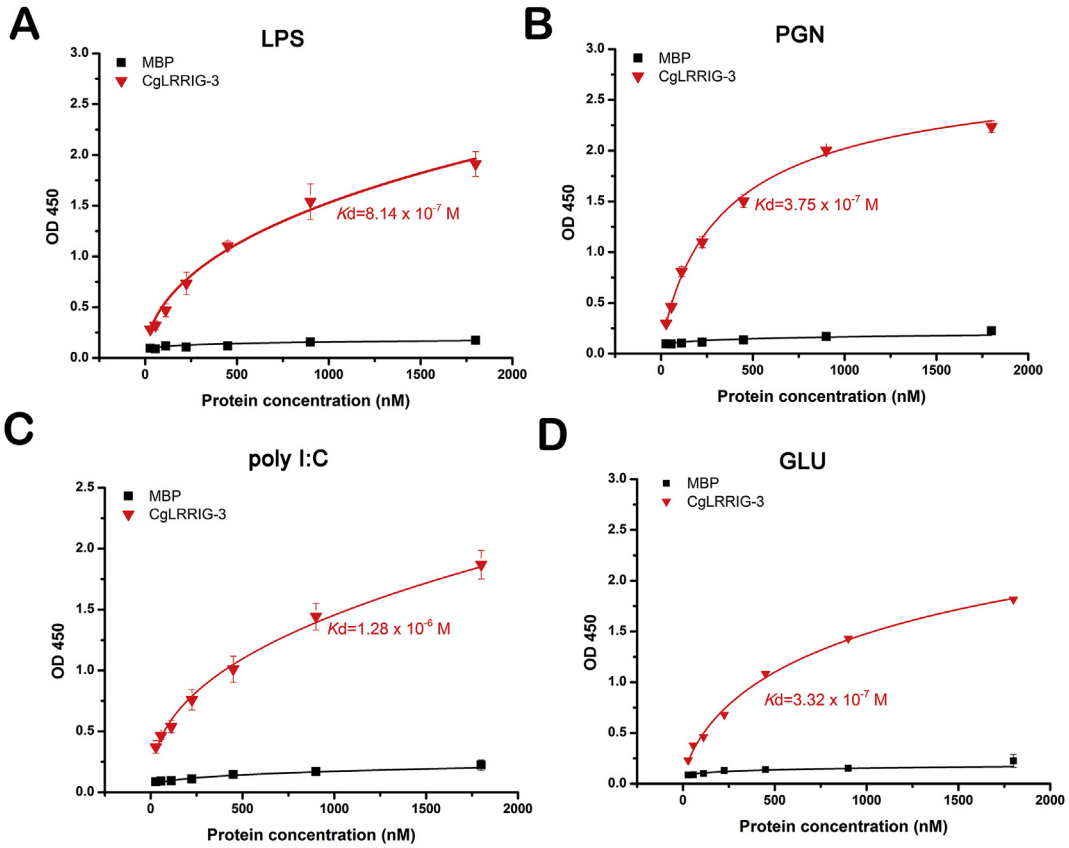


**Fig. 6.** PAMPs binding affinity of rCgLRRIG-3. A: LPS, B: PGN, C: poly I:C, D: GLU. The results were shown as mean ± S.D. (n = 3), the binding curve was fitted and the dissociation constant (Kd) was quantified based on the curve-fitted binding model.

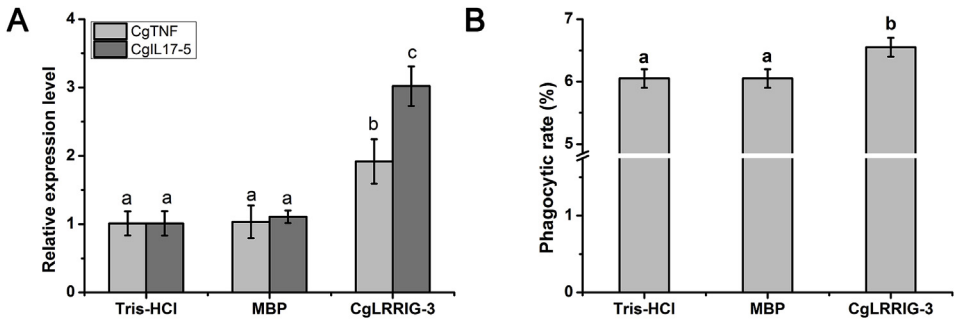


**Fig. 7.** (A) The induced mRNA expression of CgTNF-1 and CgIL17-5 in cultured oyster hemocytes by rCgLRRIG-3. (B) The induced phagocytic rate of cultured oyster hemocytes by rCgLRRIG-3.The results were shown as mean ± S.D. (n = 3), and bars with different characters indicated significantly different ($p < 0.05$).

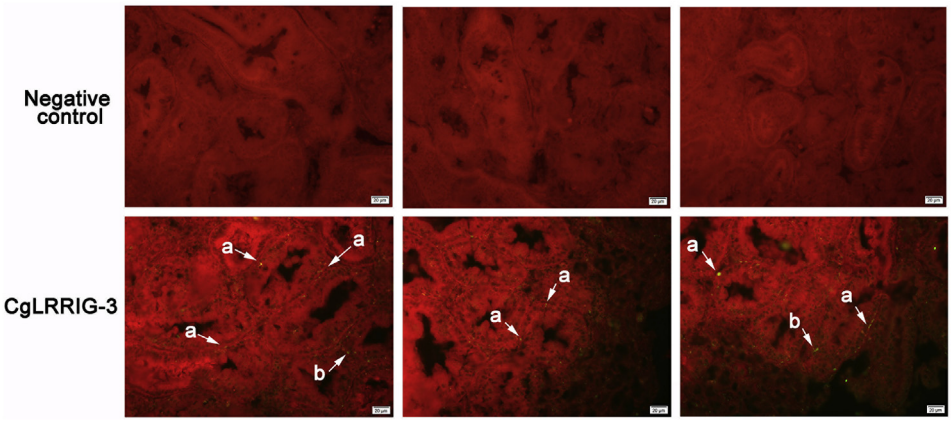


**Fig. 8.** Immunohistochemistry of CgLRRIG-3 in oyster hepatopancreas exhibiting the basolateral membrane of digestive tubule (arrow a) and the hemocoel sinusoid between the digestive tubules (arrow b). The distributions of CgLRRIG-3 were visualized by Alexa Fluor 488-labeled goat-anti-mouse antibody and the tissues were stained with Evans blue dye (red).

hemocytes were fixed with 4% PFA (Paraformaldehyde diluted in TBS) for 15 min. After washing and blocking, the fixed cells were incubated with 500 μL antibody of rLRRIG-3 (diluted 1:500 in blocking buffer) at room temperature for 1 h. With another three times of washing, the cells were incubated with Alexa Fluor 488-labeled goat-anti-mouse antibody (diluted 1:1000 in blocking buffer) at 25 °C for 1 h and 4′,6-Diamidine-2′-phenylindole dihydrochloride (DAPI, Roche, 10 mg $mL^{-1}$, diluting in PBS by 1:2500) for 5 min in dark. After the last three washing, the slides were sealed with 50% glycerol and observed with Laser Scan Confocal Microscope (LSM800, ZEISS, German).

Immunohistochemistry of CgLRRIG-3 was performed according to previous description [28]. The hepatopancreas was fixed Bouin's solution, dehydrated with 70%–100% ethanol and embedded in paraffin. After that, the tissues were cut at 6 μm thickness, followed by eliminating paraffin and rehydration in successive 95%–30% ethanol baths and water. Antigens were then refolded and the slides were blocked, incubated with primary and secondary antibody. The slides were finally stained with Evans blue dye, covered with cover slide and observed under fluorescence microscopy (Olympus).

### 2.12. Flow cytometry assay of CgLRRIG-3 in hemocytes

For flow cytometry assay of CgLRRIG-3 in hemocytes, the hemocytes were fixed in 4% PFA for 15 min and permeabilized with 0.5% Triton-100 for 5 min before blocked. Then the hemocytes were incubated with polyclonal antibody of CgLRRIG-3 (diluted by 1:500) for 3 h and Alexa Fluor 488-conjugated goat anti-mouse IgG for 1 h. After three times of washing, the stained hemocytes were detected by flow cytometry.

### 2.13. Antibody blocking of CgLRRIG-3

Hemocytes were obtained as described above and incubated with polyclonal antibody of CgLRRIG-3 (diluted 1:500 in M-L-15) for 1 h at room temperature with rotation. After three times of washing with M-L-15 medium, the phagocytosis rate of hemocytes were determined as in *2.10*.

### 2.14. Statistical analysis

All experiments were carried out in triplicate and the data were presented as mean ± S.D. (N = 3). The significant differences among groups were analyzed by SPSS 16.0 and tested by one-way analysis of variance (ANOVA) and multiple comparisons. Differences were considered significant at $p < 0.05$.

## 3. Results

### 3.1. Sequence features and phylogeny of CgLRRIG-3

The full-length cDNA sequence of CgLRRIG-3 was retrieved from NCBI in the *C. gigas* genome with GenBank accession number of XP_011429625.1. An open reading frame (ORF) of 1716 bp which encoded a polypeptide of 571 amino acids could be identified. The theoretical isoelectric point was 5.59 and the predicted molecular mass was about 65.65 kD. As shown in Fig. 1, two LRR motifs ($L_{15}$-$N_{39}$) and ($M_{40}$-$P_{63}$), a LRRNT motif ($N_{75}$—$P_{127}$), an Ig domain ($Q_{135}$-$D_{259}$) and a transmembrane domain ($F_{272}$-$A_{294}$) were found in the deduced amino acid sequence of CgLRRIG-3. No signal peptide was revealed in CgLRRIG-3. The two LRR motifs both exhibited consensus signature sequence as LxxLxLxxNxL. By PSI-BLAST algorithms, twelve proteins with LRR motifs and Ig domain were selected. In the phylogenetic tree (Fig. 2), twelve proteins were clustered into two main branches of vertebrates and invertebrates, and CgLRRIG-3 was first clustered with BgLRRIG-2 from *Biomphalaria glabrata*, which formed a sister group with LpLRRN like, DwLRRIG2, TcLRRIG from *Limulus polyphemus, Drosophila willistoni* and *Temnothorax curvispinosus*. Then CgLRRIG-3 were successively clustered with LRR motif and Ig domain containing

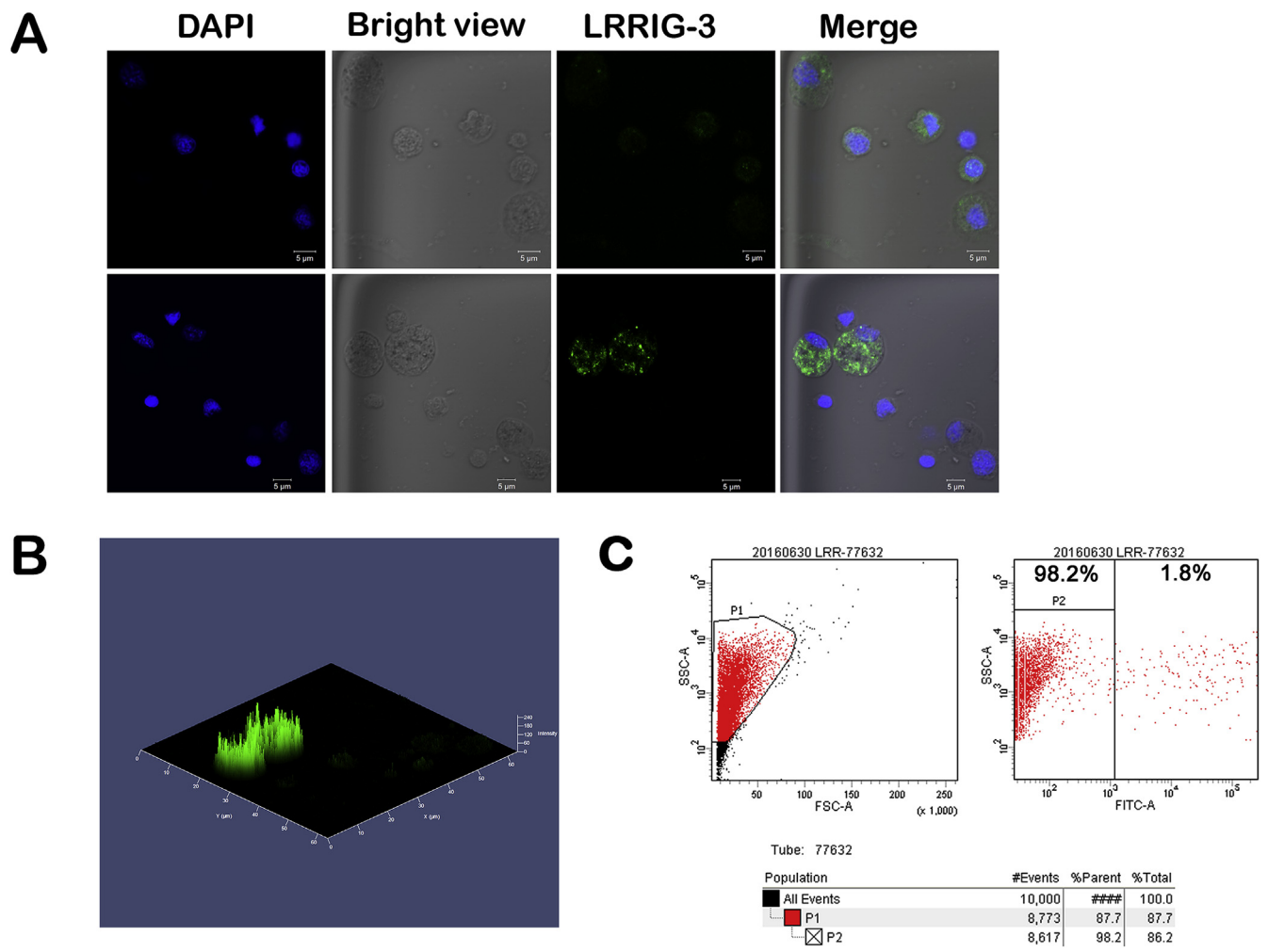


**Fig. 9.** (A) Immunohistochemistry of CgLRRIG-3 in oyster hemocytes. The distributions of CgLRRIG-3 were visualized by Alexa Fluor 488-labeled goat-anti-mouse antibody and the nuclei were stained with DAPI (blue). (B) The relative intensity of the fluorescence signal of CgLRRIG-3 in hemocytes revealed by confocal analysis. (C) Flow cytometry assay of CgLRRIG-3 polyclonal antibody and Alexa Fluor 488-conjugated goat anti-mouse IgG stained hemocytes.

proteins from *Xenopus tropicalis, Poecilia formosa, Colius striatus, Oryctolagus cuniculus, Mus musculus, Mus musculus* and finally gathered with CjLRRN1 from *Callithrix jacchus* and HsLRRN1 from *Homo sapiens*.

### 3.2. The tissue distributions of CgLRRIG-3

The relative mRNA expression levels of CgLRRIG-3 in different tissues were investigated by qRT-PCR with the CgEF gene as the internal control. The specificity of the primers for RT-PCR by analyzing the dissociation curve and there was only a peak at the melting temperature (data not shown). As shown in Fig. 3, the mRNA transcripts of CgLRRIG-3 could be detected in all the tested tissues including muscle, gill, hepatopancreas, mantle, gonad and hemocytes. The highest expression level was detected in hepatopancreas, which was 16.64-fold than that in female gonad. The relative expression levels in muscle, gill, hemocytes, mantle and male gonad were 8.41-fold, 7.44-fold, 6.50-fold, 4.92-fold and 2.54-fold of that in the female gonad, respectively.

### 3.3. The mRNA expression profiles of CgLRRIG-3 post PAMPs stimulations

The mRNA expression levels of CgLRRIG-3 in hemocytes were investigated from 3 h to 48 h after stimulation of four different PAMPs (Fig. 4). The temporal mRNA expression profiles after stimulation of four PAMPs were different. There were two peaks at 3 h (2.87-fold, $p < 0.05$) and 12 h (5.75-fold, $p < 0.05$) after LPS stimulation. After PGN stimulation, the relative expression level remained unchanged in the first 3 h and was upregulated during 6–9 h and reached the maximum at 9 h (2.20-fold, $p < 0.05$). Then it was down-regulated and revealed no significant difference with the original level at 24 h and 48 h. For poly I:C stimulation, the mRNA expression of CgLRRIG-3 was significantly up-regulated to 6.81-fold at 3–6 h ($p < 0.05$). Then it decreased during 6–12 h and came to the original level at 12–48 h. After GLU stimulation, the expression level gradually increased to the peak (2.62-fold, $p < 0.05$) from 0 to 9 h and decreased to the original level at 48 h.

### 3.4. The recombinant proteins of CgLRRIG-3 and the polyclonal antibodies

The 813 bp cDNA fragment encoding the amino acids sequences from $M_1$ to $L_{271}$ from the extracellular part of CgLRRIG-3 was cloned using primers of CgLRRIG-3-recombinant-F and CgLRRIG-3-recombinant-R. Recombinant protein of CgLRRIG-3 with a MBP tag was revealed with molecular weight of approximately 70 kD (Fig. 5, lane 6) and the purified MBP protein has a molecular weight of 40 kD. Western blotting was performed to detect the specificity of polyclonal antibody of CgLRRIG-3 and one distinct band of about 70 kD was revealed (Fig. 5, lane 7). The specificity of the antibody to homogenates of hepatopancreas and hemocytes was also investigated and two bands of about 35 kD and 65 kD were revealed (Fig. 5, lane 8, lane 9).

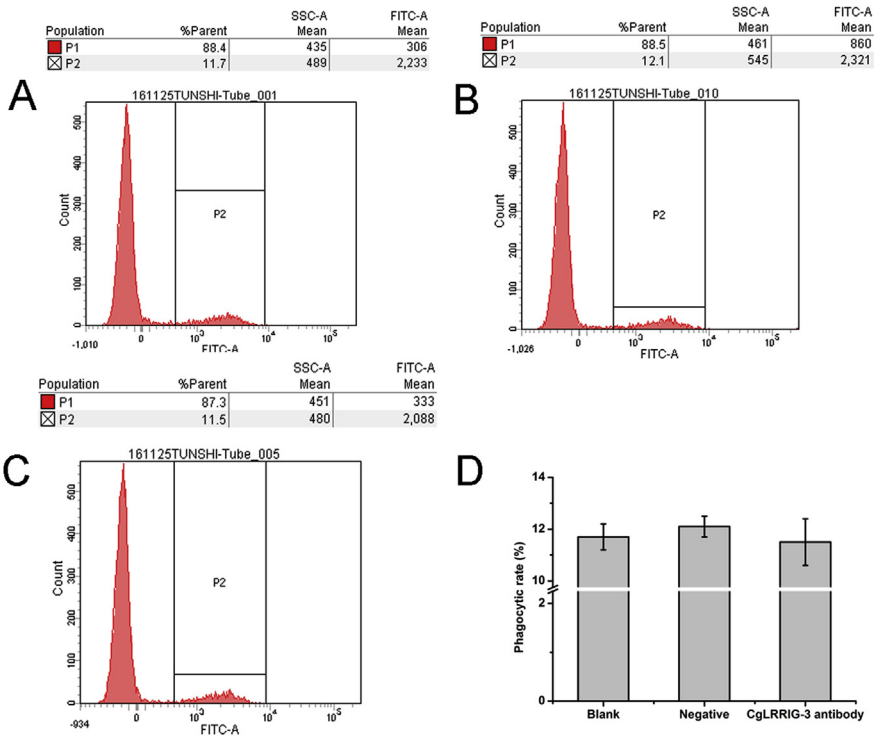


**Fig. 10.** Flow cytometry assay of hemocytes phagocytosis after blockade of CgLRRIG-3 with CgLRRIG-3 polyclonal antibody. (A) Hemocytes without treatment (blank). (B) Hemocytes treated with negative mouse serum. (C) Hemocytes treatment with CgLRRIG-3 polyclonal antibody. (D) The statistics of hemocytes phagocytosis rate. The results were shown as mean ± S.D. (n = 3), and bars with different characters indicated significantly different ($p < 0.05$).

### 3.5. The PAMP binding activities of rCgLRRIG-3

ELISA was performed to examine the binding activities of rCgLRRIG-3 to four different PAMPs. As shown in Fig. 6, rCgLRRIG-3 could bind to all the four PAMPs, including LPS, PGN, poly I:C and GLU, in a concentration-dependent manner while MBP revealed no activity at any concentrations. The apparent dissociation constants (Kd) of rCgLRRIG-3 to LPS, PGN, poly I:C and GLU were calculated to be $8.14 \times 10^{-7}$ M, $3.75 \times 10^{-7}$ M, $1.28 \times 10^{-7}$ M and $3.32 \times 10^{-7}$ M, respectively.

### 3.6. The enhancement of cytokines expression and phagocytosis rate by rCgLRRIG-3

The relative mRNA expression levels of two cytokines CgTNF-1 and CgIL17-5 were investigated after the hemocytes were incubated with CgLRRIG-3. After incubation with rCgLRRIG-3, the mRNA transcripts of CgTNF-1 were significantly up-regulated by 1.92-fold ($p < 0.05$) and that of CgIL17-5 by 3.02-fold ($p < 0.05$) (Fig. 7A). The phagocytosis rate of the hemocytes was also enhanced from 6.05% to about 6.55% ($p < 0.05$) (Fig. 7A).

### 3.7. Localization of CgLRRIG-3 in hepatopancreas and hemocytes

Immunohistochemistry was carried out to detect the localization of CgLRRIG-3 in hepatopancreas. As shown in Fig. 8, the positive signal of CgLRRIG-3 (green) was mainly located on the basolateral membrane of digestive tubule (arrow a in Fig. 8) and the hemocoel sinusoid between the digestive tubules (arrow b in Fig. 8).

In hemocytes, positive immunoreactivity of CgLRRIG-3 could be (green signal) clearly observed in cytoplasm and on the cell membrane of a group of granulocytes with diameter about 12–15 μm (Fig. 9A). The fluorescence intensity of the positive signal was much stronger than the background revealed by confocal analysis (Fig. 9B). To determine the ratio of CgLRRIG-3 positive population, flow cytometry assay of CgLRRIG-3 polyclonal antibody and Alexa Fluor 488-conjugated goat anti-mouse IgG stained hemocytes was carried out. The CgLRRIG-3 positive population (P3) accounted for about 1.80% of the whole oyster hemocytes (Fig. 9C).

### 3.8. Phagocytosis rate analysis after blockade of CgLRRIG-3 using polyclonal antibody

The phagocytosis rates of hemocytes toward FITC-labeled latex beads in the blank, negative serum blocked group and CgLRRIG-3 polyclonal antibody blocked group were 11.7%, 12.1% and 11.5% (Fig. 10), respectively, which revealed no significant difference ($p > 0.05$). The result suggested that the blockade of CgLRRIG-3 had no effect on the phagocytic rate toward latex beads.

## 4. Discussion

The LRR domain and Ig domain are extremely important molecular constituents of innate immune system from invertebrates to vertebrates [3,15,18,31]. In the past decades, a variety of proteins containing both LRR and Ig domains have been discovered and the functions of some have been verified in a series of signal pathways [19]. In invertebrates, a large number of LRRIGs have been discovered but the functions remain largely unexplored. In the present study, CgLRRIG-3 was identified from oyster and it shared structural similarities with previously identified CgLRRIG-1 and CgLRRIG-2 with an LRR domain, an Ig domain, a transmembrane region, and a C-terminal cytoplasmic tail, demonstrating it was a typical LRRIG [25]. The structure of LRR domain which consisted of only two LRR motifs and a LRRNT motif differentiated it from CgLRRIG-1 and CgLRRIG-2. By PSI-BLAST, the sequence of CgLRRIG-3 was most related with LRRN1 proteins from vertebrates, suggesting it was a novel member of LRRIGs and might play different roles. The structure of CgLRRIG-3 and its relation with LRRN1 from vertebrates indicated that it could have functions in protein-protein and protein-ligand interactions and might also play some special roles.

The mRNA transcripts distribution of CgLRRIG-3 in different tissues was detected to investigate its potential function. The result indicated that it was constitutively expressed in gill, muscle, hepatopancreas,

mantle, gonad and hemocytes, indicating the essential role of CgLRRIG-3 in multiple physiological processes of oyster. Such ubiquitous distribution corresponded to those of CgLRRIG-1 and CgLRRIG-2 in oyster [25] and the majority of LRRIG protein family from vertebrates which exhibited broad mRNA tissue-expression profiles [32]. The highest mRNA expression level of CgLRRIG-3 was found in hepatopancreas, which was also consistent with CgLRRIG-1 and CgLRRIG-2. As an important organ of immune and metabolic functions in mollusks and crustaceans, the hepatopancreas was reported as a master regulator in the innate immune response [30,33,34]. It was reported that other LRR-containing proteins such as LRR-only proteins from scallop (CfLRRop-1 to CfLRRop-5) were also demonstrated to be highly expressed in hepatopancreas [12,13,31], suggesting that CgLRRIG-3 might exhibit similar immunomodulation activities on downstream immune effectors. To demonstrate the potential roles of CgLRRIG-3 in immune responses, its mRNA transcripts in hemocytes after stimulation with different PAMPs were investigated and the result indicated CgLRRIG-3 could respond to all four kinds of PAMPs. Interestingly, the response pattern of CgLRRIG-3 was quite different from that of CgLRRIG-1 and CgLRRIG-2. The expression levels of CgLRRIG1 and CgLRRIG-2 after poly I:C stimulation were much higher than that after LPS and PGN stimulation [25]. While CgLRRIG-3 responded more intensely to both LPS and Poly I:C, demonstrating the functional diversity of LRRIG proteins in oyster during evolution.

Previously, the two identified LRRIG proteins from oyster have been demonstrated to recognize and bind to various PAMPs with high infinity and induce immune effectors including CgTNF and CgIL17-5 [25]. In the present research, CgLRRIG-3 could also bind to PGN from Gram-positive bacteria, LPS from Gram-negative bacteria, GLU from fungi and poly I:C from virus in a dose-dependent manner. At the same time, the expressions of CgTNF-1 and CgIL17-5, which were demonstrated to be important cytokines and play crucial roles in the modulation of immune response of oyster [29,30], and the phagocytic rate of the hemocytes after incubation with rCgLRRIG-3 increased significantly ($p < 0.05$). Therefore, these results demonstrated that CgLRRIG-3 might play important roles in innate immunity of oyster and function as immune effectors. But it should be noted that the apparent dissociation constants (Kd) of CgLRRIG-3 towards the four different PAMPs including LPS ($8.14 \times 10^{-7}$ M), PGN ($3.75 \times 10^{-7}$ M), poly I:C ($1.28 \times 10^{-7}$ M) and GLU ($3.32 \times 10^{-7}$ M) were almost an order of magnitude higher than that of CgLRRIG-1 which were $2.44 \times 10^{-8}$ M, $4.36 \times 10^{-8}$ M, $2.47 \times 10^{-8}$ M and $2.14 \times 10^{-8}$ M, respectively [25]. These values were also much higher when compared with that of CgLRRIG-2 to LPS ($2.95 \times 10^{-7}$ M), PGN ($3.10 \times 10^{-7}$ M), poly I:C ($1.82 \times 10^{-7}$ M) and GLU ($4.04 \times 10^{-7}$ M) [25]. These results indicated that the binding affinities of CgLRRIG-3 to these four PAMPs were much weaker than CgLRRIG-1 and CgLRRIG-2, suggesting the auxiliary role of CgLRRIG-3 in immune defense. Such auxiliary roles to immune response could also be verified by weaker ability for activation of signal transduction for the release of CgTNF-1 and CgIL17-5 than CgLRRIG-1 and CgLRRIG-2. This phenomenon might be explained by the functional differentiation of LRRIGs in oyster. As shown in PSI-BLAST result, CgLRRIG-3 was most related to LRRN1 protein in vertebrate while CgLRRIG-1 and CgLRRIG-2 were related to LRR containing protein 24 (LRRC24) [25]. Recently, the functions of some LRRN1 proteins in vertebrates were reported. For example, in chick, LRRN1 was indicated to be expressed in midbrain cells but not in anterior hindbrain cells and play potential roles in chick neural development [35,36]. And LRRC24 was demonstrated to function differently and involved in protein-protein interactions as interactors with Robo receptors [37]. Therefore, a hypothesis that LRRIGs with similar sequence structure started to differentiate in mollusk was proposed and CgLRRIG-3 might have other functions in addition to immune effectors or pro-inflammatory factors in oyster.

The immunohistochemistry of CgLRRIG-3 in hepatopancreas and hemocytes was investigated. The result revealed that the positive signal of CgLRRIG-3 was mainly distributed in the basolateral membrane of digestive tubule (arrow a in Fig. 8) and the hemocoel sinusoid between the digestive tubules (arrow b in Fig. 8). According to previous study [34], the basolateral membrane of digestive tubule was supposed to be epithelial cells, which play a central role in intermediate metabolism and anti-pathogen defense. As the first line of defense, the epithelial cells of hepatopancreas are rich in fixed phagocytes which are capable of engulfing foreign bacterial components and cellular debris from the lumen [38]. The hemocoel sinusoids, where the hemolymph pass through, also contains phagocytizing hemocytes [34]. These hemocytes may accumulate antigens and serving as a signal for the gland cells to initiate an immune response. The distribution of CgLRRIG-3 in hemocytes was further elucidated and the result demonstrated that the signal of CgLRRIG-3 was mainly observed in cytoplasm and on the cell membrane of a group of granulocytes with diameter about 12–15 μm, which account for 1.80% of the total oyster hemocytes. A previous study indicated that granular cells in circulating hemocytes of oyster usually had a median diameter of 15 μm (min. 11.5 μm; max. 18 μm) [39] and a recent study also categorized oyster hemocytes into three cell types including agranulocytes, granulocytes and semigranulocytes based on the cell size and cellular contents and granulocytes were illustrated to have larger cell size (approximate 10–14 μm) [40]. Such a distribution in hemocytes corresponded with the western blotting result of Fig. 5B that two bands of about 35 kD and 65 kD were revealed in hemocytes and hepatopancreas. The result indicated that CgLRRIG-3 might be processed proteolytically to a lower molecular weight form (35 kD) which might enter the cytoplasm and trigger cellular downstream pathways. The truncation of LRR proteins has been reported in a leucine-rich repeat (LRR) protein from tomato plants that is processed during pathogenesis [41]. To further investigate its role, CgLRRIG-3 on the surface of hemocytes was blocked and the phagocytic rate of the whole hemocytes towards latex beads remained unchanged. The result might be explained by the low proportion of this group of granulocytes. As the granulocytes were functionally characterized as the main immunocompetent hemocytes with phagocytic and encapsulating ability [42]. Another explanation might be that this subpopulation granulocytes had some specialized function which remained unknown and need further exploration. As we have demonstrated above, the sequence of CgLRRIG-3 was most related with LRRN1 proteins from vertebrates. Recently, LRRN1 protein was proved to be a new maker on human embryonic stem cells (hESCs) and play an important role in hESC proliferation, stemness and differentiation [43]. Evidences from other invertebrates such as crayfish showed that hemocytes also have stem cell-like behavior, giving rise to neurons in the cerebral ganglia [44,45]. As an ancient specie, the relationship between the neuro system and immune system have aroused researchers' interests [45]. The present results suggested that in oyster immune-related hemocytes might have the ability to differentiate to neuro-related cells and CgLRRIG-3 might be an important marker which not only have important roles in pattern recognition and cytokines induction and also specialized in a particular subpopulation of granulocytes. The precise function of CgLRRIG-3 and its relation with this subpopulation with the group of hemocytes remain unclear and await further elucidation, though.

In summary, a novel LRR domain and Ig domain containing protein (CgLRRIG-3) were identified from Pacific oyster *C. gigas*. CgLRRIG-3 is constitutively expressed in all tissues and its mRNA transcripts in hemocytes significantly increased post PAMPs stimulation. The recombinant proteins exhibited a wide PAMP binding repertoire to four typical PAMPs and could significantly induce the expression of CgTNF-1 and CgIL17-5 and increase phagocytosis in primary cultured oyster hemocytes. CgLRRIG-3 was confirmed to be hemocytes sub-population-specific and mainly distributed expressed in a special group of granulocytes. These results will not only help us to understand the characteristics of CgLRRIG-3 and its functions as an immune effector.

## Acknowledgement

This study was supported by a grant from National Natural Science Foundation of China (No. 31800414), Open Fund of Key Laboratory of Experimental Marine Biology, Chinese Academy of Sciences (No. KF2018NO1), and Research Initial Funding Project for Doctors in Qingdao University of Science and Technology (No. 010022908).

## References

[1] S. Akira, S. Uematsu, O. Takeuchi, Pathogen recognition and innate immunity, Cell 124 (4) (2006) 783–801.
[2] R. Medzhitov, Recognition of microorganisms and activation of the immune response, Nature 449 (7164) (2007) 819–826.
[3] L. Kedzierski, J. Montgomery, J. Curtis, E. Handman, Leucine-rich repeats in host-pathogen interactions, Arch. Immunol. Ther. Exp. 52 (2) (2004) 104–112.
[4] D.M. Halaby, J.P. Mornon, The immunoglobulin superfamily: an insight on its tissular, species, and functional diversity, J. Mol. Evol. 46 (4) (1998) 389–400.
[5] L. Wang, L. Qiu, Z. Zhou, L. Song, Research progress on the mollusc immunity in China, Dev. Comp. Immunol. 39 (1–2) (2013) 2–10.
[6] U. Consortium, The universal protein resource (UniProt) in 2010, Nucleic Acids Res. 38 (2010) D142–D148 Database issue.
[7] B. Kobe, A.V. Kajava, The leucine-rich repeat as a protein recognition motif, Curr. Opin. Struct. Biol. 11 (6) (2001) 725–732.
[8] A.C. Ng, J.M. Eisenberg, R.J. Heath, A. Huett, C.M. Robinson, G.J. Nau, R.J. Xavier, Human leucine-rich repeat proteins: a genome-wide bioinformatic categorization and functional analysis in innate immunity, Proc. Natl. Acad. Sci. U.S.A. 108 (Suppl 1) (2011) 4631–4638.
[9] M. Povelones, L.M. Upton, K.A. Sala, G.K. Christophides, Structure-function analysis of the Anopheles gambiae LRIM1/APL1C complex and its interaction with complement C3-like protein TEP1, PLoS Pathog. 7 (4) (2011) e1002023.
[10] J. Gong, T. Wei, Structure modeling of Toll-like receptors, Mol. Biol. Rep. (Clifton, N.J.) 1169 (2014) 45–53.
[11] A. Bej, B.R. Sahoo, B. Swain, M. Basu, P. Jayasankar, M. Samanta, LRRsearch: an asynchronous server-based application for the prediction of leucine-rich repeat motifs and an integrative database of NOD-like receptors, Comput. Biol. Med. 53 (2014) 164–170.
[12] M. Wang, L. Wang, Y. Guo, Q. Yi, L. Song, An LRR-only protein representing a new type of pattern recognition receptor in Chlamys farreri, Dev. Comp. Immunol. 54 (1) (2016) 145–155.
[13] M. Wang, L. Wang, L. Xin, X. Wang, L. Wang, J. Xu, Z. Jia, F. Yue, H. Wang, L. Song, Two novel LRR-only proteins in Chlamys farreri: similar in structure, yet different in expression profile and pattern recognition, Dev. Comp. Immunol. 59 (2016) 99–109.
[14] S. Huang, S. Yuan, L. Guo, Y. Yu, J. Li, T. Wu, T. Liu, M. Yang, K. Wu, H. Liu, J. Ge, Y. Yu, H. Huang, M. Dong, C. Yu, S. Chen, A. Xu, Genomic analysis of the immune gene repertoire of amphioxus reveals extraordinary innate complexity and diversity, Genome Res. 18 (7) (2008) 1112–1126.
[15] J.P. Cannon, L.J. Dishaw, R.N. Haire, R.T. Litman, D.A. Ostrov, G.W. Litman, Recognition of additional roles for immunoglobulin domains in immune function, Semin. Immunol. 22 (1) (2010) 17–24.
[16] F.L. Watson, R. Puttmann-Holgado, F. Thomas, D.L. Lamar, M. Hughes, M. Kondo, V.I. Rebel, D. Schmucker, Extensive diversity of Ig-superfamily proteins in the immune system of insects, Science 309 (5742) (2005) 1874–1878.
[17] S.M. Zhang, C.M. Adema, T.B. Kepler, E.S. Loker, Diversification of Ig superfamily genes in an invertebrate, Science 305 (5681) (2004) 251–254.
[18] C. Liu, S. Jiang, M. Wang, L. Wang, H. Chen, J. Xu, Z. Lv, L. Song, A novel siglec (CgSiglec-1) from the Pacific oyster (Crassostrea gigas) with broad recognition spectrum and inhibitory activity to apoptosis, phagocytosis and cytokine release, Dev. Comp. Immunol. 61 (2016) 136–144.
[19] F. Mao, B. Wang, Q. Xiao, F. Cheng, T. Lei, D. Guo, LRIG proteins in glioma: functional roles, molecular mechanisms, and potential clinical implications, J. Neurol. Sci. 383 (2017) 56–60.
[20] D. Guo, C. Holmlund, R. Henriksson, H. Hedman, The LRIG gene family has three vertebrate paralogs widely expressed in human and mouse tissues and a homolog in Ascidiacea, Genomics 84 (1) (2004) 157–165.
[21] M. Musacchio, N. Perrimon, The Drosophila kekkon genes: novel members of both the leucine-rich repeat and immunoglobulin superfamilies expressed in the CNS, Dev. Biol. 178 (1) (1996) 63–76.
[22] C.M. MacLaren, T.A. Evans, D. Alvarado, J.B. Duffy, Comparative analysis of the Kekkon molecules, related members of the LIG superfamily, Dev. Gene. Evol. 214 (7) (2004) 360–366.
[23] G. Zhang, X. Fang, X. Guo, L. Li, R. Luo, F. Xu, P. Yang, L. Zhang, X. Wang, H. Qi, Z. Xiong, H. Que, Y. Xie, P.W. Holland, J. Paps, Y. Zhu, F. Wu, Y. Chen, J. Wang, C. Peng, J. Meng, L. Yang, J. Liu, B. Wen, N. Zhang, Z. Huang, Q. Zhu, Y. Feng, A. Mount, D. Hedgecock, Z. Xu, Y. Liu, T. Domazet-Loso, Y. Du, X. Sun, S. Zhang, B. Liu, P. Cheng, X. Jiang, J. Li, D. Fan, W. Wang, W. Fu, T. Wang, B. Wang, J. Zhang, Z. Peng, Y. Li, N. Li, J. Wang, M. Chen, Y. He, F. Tan, X. Song, Q. Zheng, R. Huang, H. Yang, X. Du, L. Chen, M. Yang, P.M. Gaffney, S. Wang, L. Luo, Z. She, Y. Ming, W. Huang, S. Zhang, B. Huang, Y. Zhang, T. Qu, P. Ni, G. Miao, J. Wang, Q. Wang, C.E. Steinberg, H. Wang, N. Li, L. Qian, G. Zhang, Y. Li, H. Yang, X. Liu, J. Wang, Y. Yin, J. Wang, The oyster genome reveals stress adaptation and complexity of shell formation, Nature 490 (7418) (2012) 49–54.
[24] L. Wang, X. Song, L. Song, The oyster immunity, Dev. Comp. Immunol. 80 (2018) 99–118.
[25] X. Wang, M. Wang, Q. Xu, J. Xu, Z. Lv, L. Wang, L. Song, Two novel LRR and Ig domain-containing proteins from oyster Crassostrea gigas function as pattern recognition receptors and induce expression of cytokines, Fish Shellfish Immunol. 70 (2017) 308–318.
[26] X. Wang, M. Wang, Z. Jia, H. Wang, S. Jiang, H. Chen, L. Wang, L. Song, Ocean acidification stimulates alkali signal pathway: a bicarbonate sensing soluble adenylyl cyclase from oyster *Crassostrea gigas* mediates physiological changes induced by $CO_2$ exposure, Aquat. Toxicol. 181 (2016) 124–135.
[27] X. Wang, M. Wang, J. Xu, Z. Jia, Z. Liu, L. Wang, L. Song, Soluble adenylyl cyclase mediates mitochondrial pathway of apoptosis and ATP metabolism in oyster *Crassostrea gigas* exposed to elevated $CO_2$, Fish Shellfish Immunol. 66 (2017) 140–147.
[28] Z. Jia, T. Zhang, S. Jiang, M. Wang, Q. Cheng, M. Sun, L. Wang, L. Song, An integrin from oyster *Crassostrea gigas* mediates the phagocytosis toward *Vibrio splendidus* through LPS binding activity, Dev. Comp. Immunol. 53 (1) (2015) 253–264.
[29] Y. Sun, Z. Zhou, L. Wang, C. Yang, S. Jianga, L. Song, The immunomodulation of a novel tumor necrosis factor (CgTNF-1) in oyster *Crassostrea gigas*, Dev. Comp. Immunol. 45 (2) (2014) 291–299.
[30] L. Xin, H. Zhang, R. Zhang, H. Li, W. Wang, L. Wang, H. Wang, L. Qiu, L. Song, CgIL17-5, an ancient inflammatory cytokine in *Crassostrea gigas* exhibiting the heterogeneity functions compared with vertebrate interleukin17 molecules, Dev. Comp. Immunol. 53 (2) (2015) 339–348.
[31] M. Wang, L. Wang, Z. Jia, X. Wang, Q. Yi, L. Zhao, L. Song, The versatile functions of LRR-only proteins in mollusk *Chlamys farreri*, Dev. Comp. Immunol. 77 (2017) 188–199.
[32] S. Homma, T. Shimada, T. Hikake, H. Yaginuma, Expression pattern of LRR and Ig domain-containing protein (LRRIG protein) in the early mouse embryo, Gene Expr. Patterns 9 (1) (2009) 1–26.
[33] X. Li, Z. Cui, Y. Liu, C. Song, G. Shi, Transcriptome analysis and discovery of genes involved in immune pathways from hepatopancreas of microbial challenged mitten crab *Eriocheir sinensis*, PLoS One 8 (7) (2013) e68233.
[34] T. Rőszer, The invertebrate midintestinal gland ("hepatopancreas") is an evolutionary forerunner in the integration of immunity and metabolism, Cell Tissue Res. 358 (3) (2014) 685–695.
[35] L.C. Andreae, D. Peukert, A. Lumsden, J.D. Gilthorpe, Analysis of Lrrn1 expression and its relationship to neuromeric boundaries during chick neural development, Neural Dev. 2 (2007) 22-22.
[36] K. Tossell, L.C. Andreae, C. Cudmore, E. Lang, U. Muthukrishnan, A. Lumsden, J.D. Gilthorpe, C. Irving, Lrrn1 is required for formation of the midbrain–hindbrain boundary and organiser through regulation of affinity differences between midbrain and hindbrain cells in chick, Dev. Biol. 352 (2–10) (2011) 341–352.
[37] E. Gilsohn, T. Volk, Fine tuning cellular recognition: the function of the leucine rich repeat (LRR) trans-membrane protein, LRT, in muscle targeting to tendon cells, Cell Adhes. Migrat. 4 (3) (2010) 368–371.
[38] V. Alday-Sanz, A. Roque, J.F. Turnbull, Clearing mechanisms of *Vibrio vulnificus* biotype I in the black tiger shrimp *Penaeus monodon*, Dis. Aquat. Org. 48 (2) (2002) 91–99.
[39] F. Rebelo Mde, S. Figueiredo Ede, R.M. Mariante, A. Nobrega, C.M. de Barros, S. Allodi, New insights from the oyster *Crassostrea rhizophorae* on bivalve circulating hemocytes, PLoS One 8 (2) (2013) e57384.
[40] S. Jiang, Z. Jia, T. Zhang, L. Wang, L. Qiu, J. Sun, L. Song, Functional characterisation of phagocytes in the Pacific oyster *Crassostrea gigas*, Peer J 4 (2016) e2590.
[41] P. Tornero, M.D. Mayda E Fau - Gomez, L. Gomez Md Fau - Canas, V.Canas L. Fau - Conejero, P. Conejero V Fau - Vera, P. Vera, Characterization of LRP, a leucine-rich repeat (LRR) protein from tomato plants that is processed during pathogenesis, Plant J. 10 (2) (1996) 315–330.
[42] W. Wang, M. Li, L. Wang, H. Chen, Z. Liu, Z. Jia, L. Qiu, L. Song, The granulocytes are the main immunocompetent hemocytes in *Crassostrea gigas*, Dev. Comp. Immunol. 67 (2017) 221–228.
[43] C.H. Liao, Y.H. Wang, W.W. Chang, B.C. Yang, T.J. Wu, W.L. Liu, A.L. Yu, J. Yu, Leucine-rich repeat neuronal protein 1 regulates differentiation of embryonic stem cells by post-translational modifications of pluripotency factors, Stem Cell. (2018), https://doi.org/10.1002/stem.2862.
[44] P.G. Chaves da Silva, D.C. Benton Jl Fau - Sandeman, B.S. Sandeman Dc Fau - Beltz, B.S. Beltz, Adult neurogenesis in the crayfish brain: the hematopoietic anterior proliferation center has direct access to the brain and stem cell niche, Stem Cell. Dev. 22 (7) (2013) 1027–1041.
[45] P.G. da Silva, B.S. Benton Jl Fau - Beltz, S. Beltz Bs Fau - Allodi, S. Allodi, Adult neurogenesis: ultrastructure of a neurogenic niche and neurovascular relationships, PLoS One 7 (6) (2012) e39267.